Evaluation of transport in the lower tropical stratosphere in a global chemistry and transport model

Anne R. Douglass, Mark R. Schoeberl and Richard B. Rood

NASA Goddard Space Flight Center

Greenbelt, MD

Steven Pawson

Goddard Earth Sciences and Technology Center

University of MD, Baltimore County, MD

Abstract

Off-line models of the evolution of stratospheric constituents use meteorological information from a general circulation model (GCM) or from a data assimilation system (DAS). Here we focus on transport in the tropics and between the tropics and middle latitudes. Constituent fields from two simulations are compared with each other and with observations. One simulation uses winds from a GCM and the second uses winds from a DAS that has the same GCM at its core. Comparisons of results from the two simulations with observations from satellite, aircraft, and sondes are used to judge the realism of the tropical transport. Faithful comparisons between simulated fields and observations for O_3, CH_4, and the age-of-air are found for the simulation using the GCM fields. The same

comparisons for the simulation using DAS fields show rapid upward tropical transport and excessive mixing between the tropics and middle latitudes. The unrealistic transport found in the DAS fields may be due to the failure of the GCM used in the assimilation system to represent the quasi-biennial oscillation. The assimilation system accounts for differences between the observations and the GCM by requiring implicit forcing to produce consistency between the GCM and observations. These comparisons suggest that the physical consistency of the GCM fields is more important to transport characteristics in the lower tropical stratosphere than the elimination bias with respect to meteorological observations that is accomplished by the DAS. The comparisons presented here show that GCM fields are more appropriate for long-term calculations to assess the impact of changes in stratospheric composition because the balance between photochemical and transport terms is likely to be more correctly represented.

I. Introduction

As first discussed by *Rood et al*. [1989], constituent evolution calculated using an off-line chemistry and transport model (CTM) that is forced by meteorological fields from a data assimilation system will reproduce observed constituent variability and transport if several conditions are met. These conditions include the following: 1) that the assimilation fields reflect the actual atmospheric state; 2) that the model photochemistry is realistic; 3) that the advection scheme is sufficiently accurate that scheme numerics have little impact. If 1) and 3) are shown to be true, the approach can be used to identify and test photochemical mechanisms.

This approach has become standard during the past decade. CTMs use winds from analyses produced by the United Kingdom Meteorological Office (UKMO) [*Chipperfield et al.*, 1994; *Chipperfield et al*., 1996], by the European Centre for Medium-Range Weather Forecasts (ECMWF) [*Lefevre et al*., 1994; *Deniel et al*., 1998], and by the Goddard Earth Observing System Data Assimilation System (GEOS DAS) [*Rood et al.*,1991; *Douglass et al.*, 1997; *Kawa et al.*, 2002]. CTM simulations have been used to interpret observations from different platforms, including aircraft [*Douglass et al*.,1993; *Lefèvre et al.*, 1994]; satellite [*Geller et al.*, 1995; *Chipperfield et al.*, 1996], balloon [*Kondo et al*., 1996] and ground based instruments [*Goutail et al.*, 1999; *Chipperfield and Pyle*, 1998; *Chipperfield*, 1999, *Sinnhuber et al.*, 2000]. CTMs using assimilated winds have been used to simulate transport and buildup of pollutant from hypothetical supersonic aircraft flying in the lower stratosphere [*Weaver et al.*, 1996] and to quantify the relative contributions of transport and photochemistry to ozone changes on seasonal and longer time scales [*Chipperfield and Jones*, 1999]. Several groups are using this approach for interpretation of satellite observations of tropospheric aerosols [*Chin et al*., 2000; *Ginoux et al.*, 2001] and constituents [*Bey et al.*, 2001].

Comparisons of model and observations reveal striking similarities, and it is well known that the assimilation-driven CTMs reproduce synoptic and planetary scale variability as observed in stratospheric ozone and other constituents at middle and high latitudes. However, good agreement of observations and model for a single tracer does not imply good agreement for a second constituent with different relative vertical and horizontal gradients. For example, *Considine et al.* [2002] demonstrated that horizontal and vertical

transport in the high latitude polar winter produce good agreement between observed and modeled values for vortex N_2O throughout the northern winter 1999-2000, but poor agreement for modeled NO_y. There are additional nagging problems as well. *Douglass et al.* [1997] and *Chipperfield* [1999] show poor representation of tracer gradients particularly between tropics and middle latitudes using the Goddard Space Flight Center (GSFC) CTM with winds from GEOS DAS and the SLIMCAT CTM with winds from UKMO respectively. Both of these studies find that modeled ozone generally compares better with observations than do long-lived tracers, with the exception of a high bias between modeled and observed ozone in the summer high latitude lower stratosphere. The weak tracer gradients between the tropics and middle latitudes are consistent with the results of *Weaver et al*. [2000], who developed a climatology for the production of laminae in ozone profiles from ozonesonde profiles and found that the model produced excessive lamination in the subtropics.

For short integrations, a CTM driven by assimilated winds provides information about the meteorological conditions in which measurements are made. Such information is useful to bring together measurements of various constituents made from different platforms (e.g., balloon, aircraft, and satellite). However, a primary application for atmospheric models is to predict the future condition of the atmosphere, and assess the importance of natural and anthropogenic changes in atmospheric composition to stratospheric ozone. Assessment calculations often require long integrations, and the requirements for model performance are stringent. Ideally the model ozone evolution will match observations because the balance between transport and photochemical

processes is represented correctly. It is also necessary that the balance among photochemical processes be represented correctly for a realistic assessment calculation [*Wennberg et al.,* 1994]. Comparisons of output from long integrations with observations of reactive constituents such as ozone and long-lived constituents such as CH_4 may be made to determine if model balances are realistic.

Comparison of model fields with observations for specific meteorological conditions can only be made for a CTM using winds from a data assimilation system. *Douglass et al.* [1999] developed data based diagnostics that could be applied to constituent fields from any three dimensional model. The diagnostics were chosen to address specific aspects of transport, so that the model evaluation would be semi-quantitative and the overall impact of future model improvements could be evaluated. All discrepancies between model and observation affect the uncertainties of assessment calculations. The uncertainties in the assessment calculations that are introduced by poor agreement of various aspects of constituent transport in the face of "good agreement" for other aspects of transport are difficult to quantify.

Recently attention has focused on the use of the mean age of stratospheric air as a tool for model evaluation. The mean age, the mass weighted average of the transit times from the tropical tropopause to any given location, is a sensitive diagnostic of model transport [*Hall and Plumb,* 1994; *Hall et al.*, 1999]. Model calculations of mean age were compared with the age determined from observations of SF_6 and CO_2 as part of Models and Measurements Intercomparison II [*Park et al.,* 1999]. *Hall et al.* [1999] show that in

most models, the age of air in the middle and high latitude lower stratosphere is too young, indicating that the overall model circulation and mixing are too rapid. Young model mean ages are consistent with strong upward tropical transport and excessive transport out of the tropics, and/or excessive horizontal mixing between middle latitudes and the tropics. Thus young age in the middle and high latitude lower stratosphere is consistent with weak horizontal constituent gradients in the lower stratosphere subtropics as found by *Douglass et al.* [1997]. *Schoeberl et al.* [2002] use trajectory calculations with meteorological input from assimilations systems and a general circulation model to show how horizontal mixing and vertical transport characteristics of the meteorological fields impact the age spectrum, i.e., the distribution of parcel transit times that comprise the mean age. The age spectra determined from DAS fields differ from that computed using winds from a GCM. The age spectra for DAS fields are too broad as a result of too much exchange between the tropics and mid-latitudes and too much vertical dispersion.

The results of *Schoeberl et al.* [2002] are consistent with the problem that modeled tracer gradients between the tropics and middle latitudes are weaker than observed. These weak horizontal tracer gradients are produced by various assimilation systems, and different approaches to utilizing assimilation winds within the CTM framework do not solve the problem. *Douglass et al.* [1997] and *Chipperfield* [1999] used fields from GEOS DAS and UKMO respectively. Applications using the GSFC CTM calculate the vertical velocities from the horizontal divergence by requiring continuity, thus an excessively strong circulation and excessive horizontal mixing may contribute to the weak horizontal

gradients. The SLIMCAT model calculates vertical transport from diabatic heating; in this case the vertical transport is realistic, but excessive horizontal mixing is possible. *Waugh* [1996] used contour advection with meteorological fields from GEOS DAS, UKMO, and NCEP to examine isentropic transport from the tropics to the middle latitudes, and found that the different meteorological fields produced similar transport. The problem of too much exchange between the tropics and mid-latitudes seems to be endemic.

This study will focus on simulations using the NASA Goddard three-dimensional chemistry and transport model. Meteorological fields from two sources are used to drive the model. These are the Finite Volume General Circulation Model (FVGCM) and the FVDAS, a version of the GEOS DAS that uses the FVGCM at its core. All aspects of the CTM are identical except the meteorological data, thus the comparisons between model fields and observations can be thought of as a controlled experiment designed to determine the effect of the assimilation process on the transport. Model fields are compared with total ozone observations (Total Ozone Mapping Spectrometer (TOMS)), ozone profiles (Halogen Occultation Experiment (HALOE) on Upper Atmosphere Research Satellite (UARS) and Southern Hemisphere Additional Ozonesondes (SHADOZ)), methane profiles (HALOE) and in situ measurements of ozone and total reactive nitrogen from the NASA ER-2.

The constituent observations used in this study are described in section II. The CTM and a short description of the meteorological data sets used to drive it are described in section

III. Section IV considers comparisons of model fields with observations, focusing primarily on the lower tropical stratosphere. Comparisons of observations of methane and ozone with results from the two simulations provide a means to untangle contributions of transport and photochemistry to ozone in the lower tropical stratosphere. Conclusions are given in section V.

II. DATA

The observations used in this study are from four sources described briefly in the following subsections.

Total Ozone Mapping Spectrometer (TOMS)

Total ozone data used here are taken from the Total Ozone Mapping Spectrometer (TOMS) instrument launched on the Earth Probe Satellite in July 1996. The data are processed with the TOMS algorithm version 7 and are described by *Mc Peters et al*. [1998]. Time series of zonal mean TOMS data are compared with model values in section IV to provide a global context for the seasonal migration of the latitudes of strongest upwelling.

Halogen Occultation Experiment (HALOE)

Russell et al. [1993] describe the HALOE instrument that has measured profiles of ozone and other important gases using solar occultation from launch of the Upper Atmosphere Research Satellite in fall of 1991 until present. Approximately 15 sunrise and sunset profiles are measured daily at each of two near-constant latitudes. Profiles for ozone and

methane used here are retrieved using algorithm version 19. Vertical resolution for ozone profiles is about 2 km; the ozone mixing ratio error estimates are ~10% between 50 hPa and 1 hPa, and ~30% at 100 hPa [*Brühl et al.*, 1996]. The vertical resolution for methane profiles is about 4 km; between 50 hPa and 0.2 hPa the total error is less than 15% [*Park et al.*, 1996]. The differences between model and observations will be explored by organizing the HALOE observations to emphasize seasonal and spatial variability in the tropics and subtropics. A typical scan of the sampling latitude for HALOE sunrise or sunset observations is shown in Figure 1. There are about 25 similar periods during 1998 and 1999 when the latitude for sunrise or sunset observations on successive days sweeps from about 30^{o} in one hemisphere to 30^{o} in the other hemisphere. Such a scan will be referred to as a sweep. Each day during a sweep HALOE measures as many as 15 profiles. The latitude change during a single day is typically 3-5 degrees.

Southern Hemisphere Additional Ozonesondes (SHADOZ)

Thompson et al. [2002] describe the ozone and temperature profiles that are available through the SHADOZ network. This data set is ideal for the comparisons used here. Ozone and temperature profiles are usually reported more than once per month at participating stations. The SHADOZ temperatures are not used in the assimilation system, thus comparisons between SHADOZ, FVGCM and FVDAS temperatures show how well the assimilation process eliminates any biases between the GCM temperatures and observations. This is not possible with HALOE temperatures because the temperature profiles reported with HALOE constituent profiles are taken from the National Center for Environmental Prediction (NCEP) analyses below 35 km. NCEP and

FVDAS analyses rely on the same temperature observations, thus comparisons in the lower stratosphere between temperature profiles from HALOE and FVDAS are not independent. The high-resolution profiles of lower stratospheric ozone are also ideal for use in this paper. The temporal and spatial range sampled by the SHADOZ stations is sufficient to resolve features like the seasonal migration of the latitude of deepest upwelling seen in TOMS and HALOE data.

ER-2

In situ observations of ozone [*Profitt et al.,* 1989] and reactive nitrogen (NO_y) [*Fahey et al.,* 1989] were made during March and October 1994 from the ER-2 near 20 km as part of the 1994 Airborne Southern Hemisphere Ozone Experiment/Measurements for Assessing the Effects of Stratospheric Aircraft (ASHOE/MAESA) campaign. The data show that the interior of the tropics between 50 and 70 hPa is strongly isolated from the middle latitudes [*Fahey et al.,* 1996]. The gradient in the observed ratio NO_y/O_3 is weaker at middle latitudes and sharper in the subtropics than the gradient of either NO_y or O_3. The ratios NO_y/O_3 calculated from the CTM driven by FVDAS and FVGCM will be compared with observations. The model fields in the lower tropical stratosphere are sensitive to the CTM balance between photochemical production, upwelling and horizontal transport and mixing.

III. MODEL

The GSFC CTM solves a coupled set of constituent continuity equations. Winds and temperatures needed for transport and photochemical reaction rates are input to the

model, thus there are no feedbacks between constituents such as ozone and the meteorological fields. Photochemical production and loss are calculated using the photochemical scheme described by *Kawa et al.* [2002]. Numerical transport is calculated using a scheme described by *Lin and Rood* [1996]. A 15-minute time step is used for transport and photochemistry. The photolysis rates are calculated using temperature dependent cross sections *JPL* [2000] and reduced fluxes that are interpolated using a table lookup based on detailed radiative transfer calculations from the model of *Anderson and Lloyd* [1990]. The photolysis rates calculated in this way agree with the photolysis benchmark which was developed as part of the Atmospheric Effects of Aviation Project [*Stolarski et al*., 1995].

Meteorological input may be taken from a general circulation model (GCM) or from a data assimilation system (DAS). The general circulation model produces fields that satisfy the equations of motion; agreement of model climate with observations is an important aspect of GCM evaluation. A data assimilation system (DAS) combines information from both observations and a general circulation model (GCM). The system produces meteorological fields that draw to the observations and also satisfy the equations of motion. If the model fully represents the atmospheric physics, and the observations are accurate, the differences between the model and observations would have zero bias and conform to a Gaussian distribution. The assimilation process would account for random errors, and the overall transport characteristics from the DAS would likely be similar to the overall characteristics of the GCM. However, current GCM fields exhibit biases when compared with observations. The DAS produces meteorological

fields that draw to the observations and satisfy the equations of motion, but to accomplish this the assimilation process implicitly provides a systematic forcing of the model. This forcing will change the overall transport characteristics of the model.

The FVGCM, which was developed in collaboration with the National Center for Atmospheric Research (NCAR), uses a flux-form semi-Lagrangian transport scheme [*Lin and Rood*, 1996, 1997] and a quasi-Lagrangian vertical coordinate system [*Lin*, 1997] to ensure accurate representation of transport by the resolved-scale flow. The FVGCM has a horizontal resolution 2^o lat by of 2.5^o long, and extends to 0.01 hPa, and the daily averaged product is available to the user. Physical parameterizations in the current version of the FVGCM are from the NCAR Community Climate Model, Version 3 (CCM3), described by *Kiehl et al*. [1998].

Various versions of GEOS DAS have been used in past applications of the GSFC CTM (e.g., GEOS-1 (UARS) by *Douglass et al.*, [1997]; GEOS-1 (STRAT) by *Douglass et al.*, [1999]; GEOS-3 (Terra) by *Kawa et al.* [2002]). Improvements in the assimilation system have been accompanied by improvements in the CTM transport. There are important differences between theTerra assimilation system (GEOS-3) and the prototype system FVDAS (GEOS-4). The spatial resolution of the Terra system is 1^o lat by 1^o long horizontal grid with 48 levels compared with 2^o lat by 2.5^o long and 55 levels in FVDAS. The Terra system uses incremental analysis update [*Bloom et al.*, 1996] and retrieved temperatures from TIROS Operational Vertical Sounder (TOVS); the FVDAS used an intermittent update and assimilates TOVS-Level-1b radiances instead of NESDIS

retrieved temperatures [*Joiner and Rokke,* 2000]. The Terra system and FVDAS both use the Physical-space Statistical Analysis Scheme (PSAS) [*Cohn et al.,* 1998]. A fundamental difference is that the GCM at the core of the Terra system (and also prior systems including GEOS-1) is replaced by FVGCM in FVDAS. Figure 2 compares potential vorticity (PV) between 30°S and 30°N at 50 hPa calculated using fields from the Terra system with PV from FVDAS. The Terra PV is much noisier than the FVDAS PV, although similar features are recognizable in both fields. As noted above, the horizontal transport produced by assimilation fields typically leads to horizontal gradients that are weaker than observed in the subtropics. Because the PV from FVDAS is much smoother than the PV from Terra, we anticipated less horizontal mixing in the CTM driven by winds from FVDAS than was produced in the CTM driven by winds from Terra, particularly between the subtropics and middle latitudes.

CTM calculations have been completed using meteorological fields from all of the GEOS data assimilation systems and also with output from the FVGCM. There are differences in the distributions of the constituents calculated using winds from the different versions of GEOS DAS, and comparisons of model ozone fields with ozone sonde data are shown in the following section. The fields produced by the CTM using winds from FVDAS are closer to observations than those computed using winds from older assimilation systems. Because this paper focuses on changes in transport that result from the assimilation process, most comparisons with observations will utilize output from the CTM driven by FVGCM (here termed CTM_{FVGCM}) or FVDAS (here termed CTM_{FVDAS}).

IV. Comparisons with Observations

Temperature, Mean Age, and Tropical Isolation

The zonal monthly mean temperature fields for January 1998 from FVDAS and the difference between FVDAS and FVGCM for 45°S – 45°N are given in Figure 3. The FVGCM is warmer in the tropical lower stratosphere than FVDAS. This comparison provides a sense of the horizontal and vertical extent of the difference between the two fields. The time series of the difference between zonal mean temperatures from FVGCM and FVDAS for the equator between 100 hPa and 10 hPa is given Figure 4a. The time series of the difference in zonal mean zonal wind from FVGCM and FVDAS at the equator is given in Figure 4b. The importance of the quasi-biennial oscillation (QBO) is evident in these difference fields. Both temperature and wind information are combined with the GCM in the assimilation process; the assimilated fields must satisfy the equations of motion and account for the physical forcing that leads to the observed evolution of wind and temperature that is absent from FVGCM. The equatorial thermal wind relationship illustrates the success of the assimilation system in producing fields that satisfy the equations of motion

$$\bar{u}_z = - \frac{R}{\beta H} \bar{T}_{yy} \qquad (1)$$

Here u is the zonal wind, T is the temperature subscripts y and z indicate the partial derivative with respect to latitude and altitude respectively, R is the dry air gas constant, H is the scale height (7 km), and β is the rate of change of the Coriolis parameter with latitude. The overbar indicates the zonal mean. This relationship is satisfied for fields

from FVGCM (not shown) since the GCM fields are solutions to the equations of motion. Time series for $\bar{u}_z$ and $-R/\beta H\ \bar{T}_{yy}$ calculated using monthly mean zonal wind and temperature show that this relationship is also satisfied for FVDAS fields (Figures 4c and 4d). However, the forcing to produce the spatial and temporal structure found in FVDAS is lacking in FVGCM. The structure is produced by the assimilation system through the input of observations; in the absence of observations the system would relax to the nearly constant easterly winds of the FVGCM. The assimilation system produces fields that are very different from the FVGCM fields but still satisfy the equations of motion in the tropics by including systematic forcing as required by the observations through the assimilation system.

To illustrate the effect of the assimilation system on the temperature distribution, histograms of the differences between temperatures at 46 hPa measured by the SHADOZ sonde network and temperatures from the FVGCM and the FVDAS at the sonde locations are shown in Figure 5. The temperatures from the FVGCM are biased with respect to the sonde temperature, while those from FVDAS compare closely with the sonde temperatures. The difference mean (-0.11K) and standard deviation (3.03K) of between sonde temperatures and FVDAS temperatures are much smaller than the difference mean (-2.13 K) and standard deviation (3.52K) between sonde temperatures and FVGCM temperatures.

The forcing in the assimilation system that is required for consistency between the observations and the GCM forecast can be considered an artificial source of heating and

momentum that will be accompanied by changes in model transport. We illustrate the changes using the mean age as a diagnostic of the integrated model transport and the isolation of the tropics from the middle latitudes.

As discussed by *Hall et al*. [1999], the mean age at a location in the stratosphere for a constituent such as SF_6 with a steady tropospheric trend is the difference between the time of a measurement and the time in the tropospheric time series when the measured value matches the troposphere value. The age of air is determined using CTM_{FVGCM} and CTM_{FVDAS} simulations of SF_6. Results are shown in Figure 6. The integration was continued until comparison of successive years showed that the age distribution had converged (nine years of simulation for CTM_{FVGCM} and five years of simulation for CTM_{FVDAS}). There are large differences between these two calculations. The stratospheric air is much younger for the CTM_{FVDAS} than for the CTM_{FVGCM}. Above 25 km, the age of air for CTM_{FVGCM} changes much more rapidly between the middle latitudes and the tropics than that for CTM_{FVDAS}. Observations suggest that at 65^{o}N the mean age should be between four and six years at 20 km. Here the age of air from CTM_{FVGCM} is greater than three years, compared with less than two years from CTM_{FVDAS}. The mean age from CTM_{FVGCM} does not reproduce all of the features of the observations, however, it is much more representative of the observations than the mean age from CTM_{FVDAS}. Note that the mean age is also sensitive to advection numerics, resolution, and choices such as use of instantaneous winds rather than time average or an on-line calculation [*Eluszkiewicz et al.*, 2000]. *Schoeberl et al.* [2002] show striking differences in results for age spectra calculated from the same wind fields using diabatic trajectories, kinematic trajectories,

and a CTM. Their result implies that there is some uncertainty in the absolute age estimate; however, the same methodology was used for the CTM_{FVDAS} and CTM_{FVGCM} calculations shown here. The methodology may affect the comparison of results from either calculation with observations, but will have little impact on comparisons between the calculations. The differences between the age distributions in Figure 6 result solely from differences in the transport produced by the FVDAS and FVGCM winds.

Fahey et al. [1996] show that the sharp gradient in the ratio NO_y/O_3 calculated from distributions of NO_y and O_3 measured from the ER-2 as part of ASHOE MAESA marks the boundary between the inner tropics and middle latitudes. The gradient at the edge of the tropics is sharper in the northern hemisphere during March and October 1994 than that in the southern hemisphere. In the northern hemisphere the steepest gradient in October is poleward of its March latitude. *Fahey et al.* [1996] reported poor agreement of the observed steep horizontal gradients with those produced by two-dimensional models available at that time, although better agreement was obtained when model diffusion was reduced to emulate the conceptual model known as the tropical pipe [*Plumb*, 1996]. The time series of the zonal mean ratio NO_y/O_3 and the absolute value of the latitudinal derivative, both at 500K, are shown in Figure 7. The contrast between the subtropics and middle latitudes is marked in CTM_{FVGCM} compared to CTM_{FVDAS}. The latitudinal gradients (Figure 7c and 7d) highlight the difference in isolation. However, both simulations reproduce the observed seasonal migration of the latitude of the steepest gradient in the northern hemisphere. The latitude of the steepest gradient varies less with season in the southern hemisphere.

The NO_y and O_3 from CTM_{FVGCM} and CTM_{FVDAS} are interpolated linearly in latitude, longitude and log pressure in the vertical, to compare the ratio NO_y/O_3 directly with the ER-2 data taken March 20-29, 1994. These results, along with the model zonal mean ratios at 56 hPa and 67 hPa, are shown in Figure 8. The apparent sharp boundary observed at 18°S reflects the vertical gradient of the ratio between 50 and 65 hPa. Ignoring this sharp transition, the CTM_{FVGCM} ratio reflects most of the features of the observations. One flight shows lower, near tropical values in the northern subtropics. Inspection of model fields shows no evidence of such variability in CTM_{FVGCM}. The CTM_{FVDAS} for 1998 or 1999 shows much weaker gradients than observed in either hemisphere. Near the equator the minimum is too large and at middle latitudes the maxima are too small. The transition between the northern subtropics and middle latitudes is less pronounced during 1999 (QBO westerly) than in 1998. This lack of agreement shows that the model balance between horizontal mixing and vertical advection is not realistic.

Comparisons of Model Total Ozone with TOMS Observations

Time series of the zonal average total ozone and the latitudinal derivative from TOMS, CTM_{FVGCM} and CTM_{FVDAS} are shown for 40°S – 40°N in Figure 9. Both simulations bear a resemblance to TOMS. The ozone in the tropics is somewhat lower in CTM_{FVDAS} than in CTM_{FVGCM} (or TOMS), suggesting that the tropical upwelling and the overall strength of the residual circulation are stronger in CTM_{FVDAS} than in CTM_{FVGCM} [*Jackman et al.*, 1991]. CTM_{FVGCM} represents the poleward migration of the low values during autumn of

the both hemispheres more faithfully than CTM_{FVDAS}. This is also demonstrated by comparison of the absolute values of the latitudinal derivatives between 40°S and 40°N. The TOMS derivative at 20°S exhibits seasonal variation; the gradient of column O_3 is weaker in Feb/Mar/Apr than between August and November. In CTM_{FVDAS}, the gradient at 20°S is nearly constant until late November. In CTM_{FVGCM}, the gradient is weaker at 20°S during June and July than in the second half of the year, and is more similar to TOMS than CTM_{FVDAS}. In the northern hemisphere, both simulations approximate the seasonal variation in TOMS, although the derivative near 20°N from CTM_{FVDAS} is too strong throughout the year. The areal extent of very weak latitudinal derivative is smaller in CTM_{FVDAS} than in the CTM_{FVGCM} or TOMS. However, in the tropics the CTM_{FVGCM} derivative shows structure not seen in the observations, and CTM_{FVGCM} values are generally higher than observed.

Histograms of the distributions of 1998 TOMS and column ozone for 15°S-15°N, and latitudes between 15° and 40° are given in Figure 10. The TOMS data are averaged into 4° latitude by 5° longitude resolution, and grid boxes with missing data are eliminated from the model fields. The most probable values, means and standard deviations of the distributions are also provided on Figure 10.

There are differences and similarities in the observed and modeled distributions. The CTM_{FVDAS} mean is close to the TOMS mean and lower than the CTM_{FVGCM} mean, consistent with stronger upwelling in CTM_{FVDAS} than CTM_{FVGCM} [*Jackman et al.*, 1991] and with the younger age of air in CTM_{FVDAS} than CTM_{FVGCM}. The distributions from

CTM_{FVDAS} and CTM_{FVGCM} do not reproduce the double peaked structure exhibited by TOMS. The distribution from CTM_{FVDAS} is broader than that from CTM_{FVGCM}. The model distributions for $15^{o} – 40^{o}$ latitude differ, and the distribution for the simulation driven by CTM_{FVGCM} is more similar to the observed distribution. Total ozone greater than 400 DU is much more probable in the CTM_{FVDAS} simulation than observed. The most probable value of the CTM_{FVDAS} distribution is 15 DU (5%) greater than that of the observed distribution, and the standard deviation is 12.3 DU (43%) greater.

Comparisons of Model Ozone with SHADOZ data

Histograms for the partial ozone column between 140 hPa and 57 hPa calculated from the ozonesondes and both models are shown in Figure 11. The distributions are divided by latitude; sonde stations between 18^{o}-26^{o}S are subtropics (340 profiles) and those between 14^{o}S and 6^{o}N (391 profiles) are tropics. The ozonesondes and CTM_{FVDAS} show similar variability in the tropics, and virtually identical standard deviations (~4.5 DU). The mean and most probable values of the distributions for the tropics using CTM_{FVDAS} or CTM_{FVGCM} are about 5 DU greater than those of the sonde distribution. The sonde distribution in the subtropics is shifted about 2 DU to higher values relative to that for the tropics. Both distributions are sharply peaked. For CTM_{FVGCM}, the subtropics distribution is shifted about 5 DU relative to the tropics and the shapes of the distributions in the tropics and subtropics are similar. The distribution from CTM_{FVDAS} bears little resemblance to that observed in the subtropics.

However, there has been improvement in the quality of simulations obtained with successive data assimilation systems, as illustrated by the distributions for simulations using winds from the TRMM (GEOS-2) and Terra data assimilation systems, also given in Figure 11. These partial columns calculated using the same model but different meteorological input show even greater variability in the subtropics relative to the tropics than CTM_{FVDAS}. Furthermore, the tropics exhibit far more variability than that observed or found in CTM_{FVDAS}. The expectation that the smoother potential vorticity for FVDAS shown in Figure 2 would be accompanied by more realistic transport is realized, but large differences remain.

Tropical ozone from either CTM_{FVDAS} or CTM_{FVGCM} is high biased when compared with sondes and with total column ozone from TOMS. The total column comparison is actually worse than it appears because the simulated column ozone should be systematically low with respect to TOMS in the tropics because TOMS contains contributions from the troposphere that are absent from the CTM. It is not possible that changes in the residual circulation can resolve all the discrepancies between observations and the model, because an increase in the strength of the upwelling or increase in the latitude breadth of upwelling that would bring the CTM ozone into better agreement with observations would surely further degrade the age of air calculation. Despite the larger upwelling in the tropics in FVDAS relative to FVGCM, the most probable ozone value of CTM_{FVDAS} is significantly higher than that of the ozonesondes. A problem with ozone photochemistry may contribute to this bias; further discussion will follow comparisons of modeled methane and ozone with that observed by HALOE.

Comparison of Ozone and Methane with HALOE Observations

The HALOE data for 1998 and 1999 are organized according to sweeps (see Figure 1) for comparisons with the model ozone and methane to illustrate the seasonal variation in the tropics. The HALOE mixing ratios for each sweep are shown as functions of latitude in Plates 1 and 2. Model sweeps are obtained by sampling the model output following the HALOE pattern and are also given in Plates 1 and 2. The differences between observed and modeled sweeps are also given in these Plates to facilitate the comparision. Note that the comparisons for each year are shown separately to emphasize differences between the two years that may be due to the QBO. The sweeps are identified by the colors of the plotting symbols; the months during which the sweeps take place are given on the bottom of the figure. The mean and standard deviation are provided for all observations that fall between 15^{o}S-15^{o}N for each year and for observations between between 15N-40N or 15S-40S in Table 1 (ozone) and Table 2 (methane).

HALOE O_3 (Plates 1a and 1f) and CH_4 (Plates 2a and 2f) show little seasonal variation during 1998 or 1999 between 15^{o}S and 15^{o}N. However, some interannual differences are apparent. In 1999 (QBO westerly), HALOE ozone between 15^{o}S and 15^{o}N is elevated compared with 1998 (QBO easterly) (compare Plates 1b and 1a). This is consistent with the lofting during the QBO easterly relative to QBO westerly as suggested by analysis of aerosol observations reported by *Trepte and Hitchman* [1992]. HALOE methane does not exhibit a signature related to the phase of the QBO at this pressure because its vertical gradient is near zero.

Seasonal variation is apparent at higher latitudes. South of 15°S the HALOE O_3 (CH_4) is higher (lower) during winter (July, September) than summer (December, March). This seasonal signature is seen in both years of HALOE observations and is apparent in O_3 and CH_4 from CTM_{FVGCM}(Plate 1b-1g and Plate 2b-2g) but not in CTM_{FVDAS} (Plate 1d-1i and Plate 2d-2i).

North of 15°N both seasonal and interannual differences are apparent. The March 1998 ozone mixing ratios are the largest observed by HALOE during this period, and the December 1998 mixing ratios are the lowest seen in 1998. In contrast, the December 1999 ozone mixing ratios exceed the March 1999 mixing ratios. The methane mixing ratios behave opposite to ozone mixing ratios because the spatial gradients of methane are opposite to those of ozone, e.g., the December 1999 mixing ratios are the lowest. The seasonal signatures for methane are much less pronounced than for ozone because the methane gradients are small relative to the ozone gradients.

As shown in the comparisons of temperature with observations, the QBO is evident in the wind fields produced by FVDAS, but the FVGCM does not produce a QBO thus the QBO is forced by observations. During 1999 the zonal wind near 46 hPa is westerly (Figure 4b), and the variance in constituent fields calculated using CTM_{FVDAS} is increased at all latitudes relative to that seen in CTM_{FVDAS} fields during 1998 (compare Plate 1e with Plate 1j and Plate 2e with Plate 2j) . Since the GCM zonal winds are always weak easterlies, the increase in variance may indicate a relationship between the noise in model

constituent fields and the difference between the base state of the GCM used in the assimilation and the observed state. The variance in CTM ozone at 46 hPa (Table 3) is largest during the westerly phase of the QBO when the difference between the GCM wind field and the observations is largest (Figure 4b). The standard deviations of the HALOE observations for ozone (Table 3) and methane (Table 4) are nearly the same for the two years within each latitude regions.

Table 1 Mean and standard deviation of HALOE ozone for 1998 and 1999 within specified latitude bands and ozone fields from CTM_{FVDAS} and CTM_{FVGCM} sampled as by HALOE

	$15^oS - 15^oN$			
	1998		1999	
	mean	σ	mean	σ
HALOE O_3	1.4 ppmv	0.23 ppmv	1.7 ppmv	0.20 ppmv
CTM_{FVDAS} O_3	1.7 ppmv	0.35 ppmv	1.9 ppmv	0.50 ppmv
CTM_{FVGCM} O_3	1.9 ppmv	0.24 ppmv	1.8 ppmv	0.23 ppmv
	$30^oS - 15^oS$ and $15^oN - 30^oN$			
	1998		1999	
	mean	σ	mean	σ
HALOE O_3	1.9 ppmv	0.41 ppmv	1.8 ppmv	0.39 ppmv
CTM_{FVDAS} O_3	2.4 ppmv	0.54 ppmv	2.4 ppmv	0.57 ppmv
CTM_{FVGCM} O_3	2.2 ppmv	0.39 ppmv	2.2 ppmv	0.36 ppmv

Table 2 Same as Table 1 for methane

	$15^oS - 15^oN$			
	1998		1999	
	mean	σ	mean	σ
HALOE CH_4	1.62 ppmv	0.07 ppmv	1.64 ppmv	0.08 ppmv
CTM_{FVDAS} CH_4	1.62 ppmv	0.05 ppmv	1.63 ppmv	0.05 ppmv
CTM_{FVGCM} CH_4	1.63 ppmv	0.03 ppmv	1.63 ppmv	0.03 ppmv
	$30^oS - 15^oS$ and $15^oN - 30^oN$			
	1998		1999	
	mean	σ	mean	σ
HALOE CH_4	1.48 ppmv	0.11 ppmv	1.45 ppmv	0.12 ppmv
CTM_{FVDAS} CH_4	1.52 ppmv	0.08 ppmv	1.53 ppmv	0.07 ppmv
CTM_{FVGCM} CH_4	1.48 ppmv	0.06 ppmv	1.42 ppmv	0.11 ppmv

HALOE methane in the subtropics and middle latitudes falls off relative to the tropics due methane loss processes at higher levels combined with both horizontal and vertical transport. The comparison of CH_4 from CTM_{FVGCM} with HALOE CH_4 suggests an appropriate balance in FVGCM. Plates 2c-2h shows no latitude dependence difference between observed and calculated methane. The increased spread in the difference at latitudes greater than 15^o is not unexpected since the FVGCM does not correspond to a particular year. Plates 2e-2j show no bias between HALOE CH_4 and that from CTM_{FVDAS} in the tropics, but bias for latitudes greater than 15^o. The difference between the average methane between 15^oS and 15^oN and the average methane between 15^o and 30^o is nearly

30% smaller for CTM_{FVDAS} than for HALOE or CTM_{FVGCM} (Table 4). This is consistent with stronger upwelling in FVDAS than FVGCM. The descent of lower methane air is also expected to be stronger, but the methane vertical gradient is weak and the excess horizontal transport is dominant.

The ozone comparisons and the age of air differences can also be explained by stronger upwelling in FVDAS than FVGCM between 15°S and 15°N. Plates 1e-1j show a smaller bias relative to HALOE O_3 between 15°S and 15°N for O_3 from CTM_{FVDAS} than from CTM_{FVGCM} (Plates 1c-1h). The decrease in the ozone bias is a result of the stronger circulation; the improved ozone comparison is countered by degraded comparisons for methane and the age of air. Note that the ozone bias in the subtropics is larger for CTM_{FVDAS} (Plates 1e-1j) than for CTM_{FVGCM} (Plates 1c-1h). Excessive downward transport acting on the steep O_3 vertical gradient contributes to the ozone overestimate at middle latitudes.

Implications for Model Photochemistry

Between 15°S – 15°N and 100-46 hPa the seasonal change in O_3 is small. The most important terms in the continuity equation are production (increases O_3) and vertical advection (decreases O_3) [*Ko et al.*, 1989; *Avallone and Prather*, 1996]. The seasonal change in tropical CH_4 is also small. In the tropical lower stratosphere, CH_4 loss is nearly negligible. In the subtropics, the mean of the observed methane distribution is significantly smaller than that in the tropics. The breadth of the distribution in subtropical methane is produced by latitudinal migration of the region of the strongest

vertical advection. Plate 2 shows that CTM_{FVGCM} reproduces many aspects of the seasonal cycle in HALOE CH_4. Even in the subtropics, the root mean square difference between model and observations is small compared with the standard deviation of the observations. In contrast, CH_4 from CTM_{FVDAS} is systematically high biased with respect to observations for latitudes greater than 15^o.

Probability distribution functions (PDFs) for ozone and methane at 46 hPa from HALOE and from both simulations are shown in Figure 12. Each panel contains PDFs determined from tropical and subtropical observations. All observations during 1998 and 1999 within the specified latitude limits are grouped together (more than 1500 observations in the tropics, more than 2300 observations between 15 and 40). For CH_4 at 46 hPa, the distributions from HALOE are similar to the distributions from the two simulations. The CH_4 vertical gradient is very weak, thus this comparison provides no information about the vertical motion. In the subtropics, the HALOE distribution is broader than that of the simulations, and the mean value and standard deviation of the HALOE distribution (1.48 ppmv, 0.1 ppmv) are more similar to those for CTM_{FGGCM} (1.44 ppmv, 0.084 ppmv) than for CTM_{FVDAS} (1.53 ppmv, 0.065 ppmv). This comparison is consistent with excess horizontal transport and mixing between the tropics and the middle latitudes.

A high bias in modeled ozone is found in the tropics and in the subtropics for both simulations. In the tropics, the mean of the ozone distribution from CTM_{FVDAS}(1.79 ppmv) is somewhat closer to the HALOE mean (1.55 ppmv) than that of CTM_{FVGCM} (1.87 ppmv). Ozonesonde values are also closer to those calculated using CTM_{FVDAS} than to

those calculated using CTM_{FVGCM}. It is not possible to bring modeled O_3 into agreement with observations without degrading the comparisons for CH_4 and the age of air. The ozone comparisons are consistent with the conclusion that the circulation in CTM_{FVGCM} is realistic but too strong for CTM_{FVDAS} if there is also a small error in stratospheric ozone production. We summarize chain of reasoning that supports this conclusion:

1. To bring the FVDAS ozone into agreement with observations in the tropics, it would be necessary to increase the tropical upwelling. Although this possibility is not eliminated by the methane comparisons (because of its weak vertical gradient), an increase in tropical upwelling would lead to even younger tropical stratospheric air.
2. CTM Ozone and CH_4 have opposite horizontal and vertical gradients in the tropics and subtropics, and the mixing ratios of both exceed observations in the subtropics. It is not possible to produce simultaneous agreement for these two constituents by changing the balance of transport processes.
3. If modeled ozone production were excessive, there would be two effects. The first would be that local ozone would be too high – if the upwelling in FVGCM is correct and feedbacks are neglected, the inferred error in production would be about 25%. The second would be that transport to the middle latitudes would be excessive by the same percentage. Reducing the production in the lower stratosphere would improve agreement of ozone from FVGCM with observations in the tropics and subtropics without affecting the good agreement already present for methane and for the age of air.
4. The ratio NO_y/O_3 for FVGCM agrees fairly well with observations (Figure 8). A small decrease in the O_3 would be accompanied by a small decrease in NO_y, since the

growth in NO_y from the tropopause to ER-2 altitudes is controlled by local production through reaction of N_2O with $O(^1D)$ and vertical advection. Thus it is expected that such a change in production would not place the model ratio NO_y/O_3 outside the range of the observations.

The production of ozone through photolysis of O_2 may be excessive for a simple reason – the CTM tropical ozone at about 2 hPa is (20%) lower than observed by HALOE, at least partly because the CTM mixing ratio for NOx ~ NO + NO_2 + 2 N_2O_5 is ~40% higher the sunset HALOE NO + NO_2 at the same pressure. The optical depth of ozone is too small, allowing for excess penetration of radiation contributing to photolysis of O_2. Such complex interactions among processes emphasize the requirement for scrupulous global evaluation of assessment models.

Discussion and Conclusions

CTMs driven by assimilated winds have played an important role in the interpretation of observations of stratospheric constituents from all platforms. However, this does not guarantee that the transport produced in a decadal scale assessment calculation will meet the stringent requirements for a meaningful assessment calculation. The comparisons shown here highlight some of the problems with the transport produced by these systems, and have implications both for future applications of CTMs such as this one and for improvements in the assimilation system. Model transport in the tropics and subtropics from CTM_{FVDAS} is shown to differ significantly from that produced by CTM_{FVGCM}, and the

transport from CTM_{FVGCM} is found to be more realistic. *Douglass et al.* [1999] developed objective criteria for evaluating transport from three sets of meteorological fields, and also found that more realistic transport was produced by winds from a general circulation model than by winds from an assimilation system. For multi-year assessment calculations, the internal consistency provided by winds and temperatures from a general circulation may be more important than representation of particular transport events using winds from a data assimilation system.

In current assimilation systems, adjustments are made to the prognostic quantities such as temperature, wind, and moisture. Other parameters such as diabatic heating and precipitation respond to these adjustments. Data assimilation techniques assume that the observations and model are unbiased. The comparisons made in this study show that the impact of the data insertion is significant where there is bias between model and observations. *Dee and da Silva* [1998] and *Dee and Todling* [2000] have studied techniques to correct bias based on observational information within a three-dimensional variational assimilation system. *Griffith and Nichols* [2000] have studied the problem of correction of systematic errors within a four-dimensional variational framework. These studies show that bias can be accommodated during the assimilation process. However, the physical or discretization errors that are responsible for the generation of the bias in the first place are not corrected. The impact on derived quantities is seen when the assimilated fields are used in applications such as CTM simulations that rely on their integrated consistency.

Thus, flaws in the tropical transport similar to those shown here are likely to be similar for any assimilation system unless the GCM at the core of the system does not exhibit systematic bias with respect to observations. The comparisons shown here emphasize the QBO, and suggest that overall transport from a CTM driven by assimilation will be flawed if the underlying GCM lacks the physical processes necessary to produce a QBO. It is likely that any systematic bias will impact the transport produced by an assimilated wind fields, however, a bias in the tropics will have a larger impact on the global transport than a bias of similar magnitude at higher latitude due to the greater area and mass involved in the tropics. Finally we note that the apparent excessive tropical transport diagnosed by tracer studies in this paper is consistent with the results of the trajectory studies of the FVDAS performed by *Schoeberl et al.* [2002].

As shown here, it is possible to use tracers along with ozone and the CTM response to changes in transport to achieve what has long been promised for CTM's driven by assimilated wind fields, i.e., to identify flaws in constituent behavior that are consistent with problems in model photochemistry. The analysis described here depends on the comparison between the results from CTM_{FVDAS} and CTM_{FVGCM} as well as the comparisons with observations, and could not be completed with a single simulation driven by assimilated winds. Finally, we emphasize that excess horizontal mixing is as detrimental to the quality of a simulation as overly vigorous vertical transport because this also upsets the balance between the transport and photochemical terms. It remains a challenge for assessment models to demonstrate that the appropriate balance between photochemical and transport contributions to continuity equations is maintained at all

latitudes and altitudes. For constituents like ozone it is also necessary to demonstrate appropriate balance among contributing photochemical processes. Development of a general circulation model that will not exhibit persistent bias with respect to meteorological observations is necessary (but not sufficient) to realize the potential contributions of assimilated datasets to assessments of trace gas transport.

Acknowledgments. We thank S.-J. Lin and Arlinda da Silva for access to the results of the FVGCM and the FVDAS. This work was supported by NASA's Atmospheric Chemistry Modeling and Analysis Program and the EOS IDS Program.

FIGURES

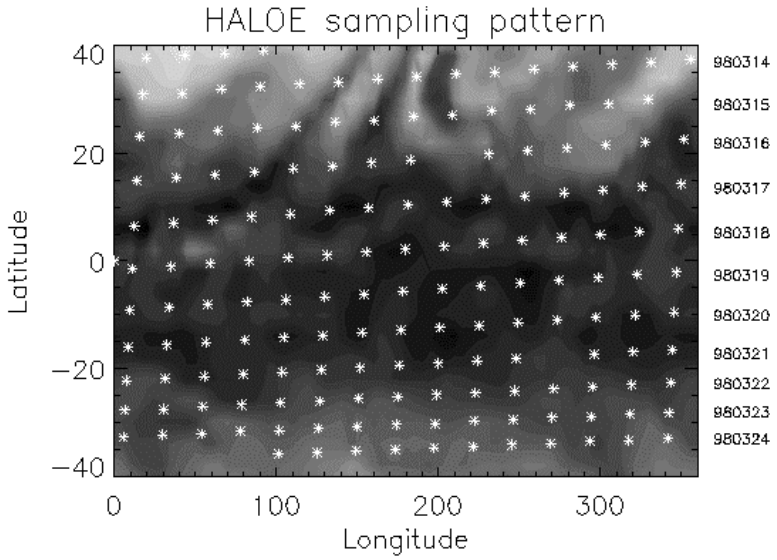

Figure 1 The locations of HALOE observations between 980314 and 980324 are superimposed on ozone at 46hPa from CTM_{FVGCM}. A group of measurements for which latitude progresses from about 30º latitude in one hemisphere to the same latitude in the opposite hemisphere is called a “sweep.”

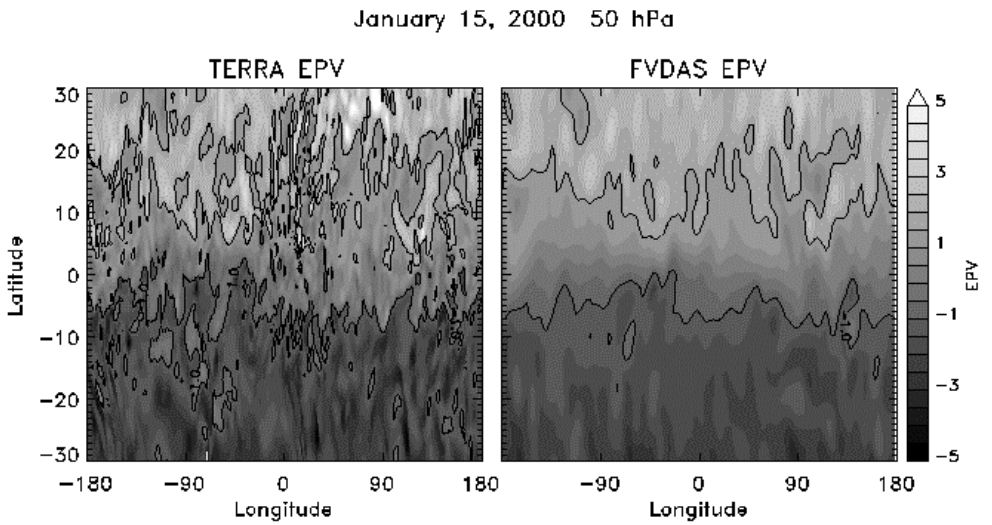

Figure 2 Potential vorticity (PV) at 50 hPa is given (a) from the Terra system and (b) from the FVDAS system. Main features are similar, but the FVDAS PV field is much smoother that from Terra.

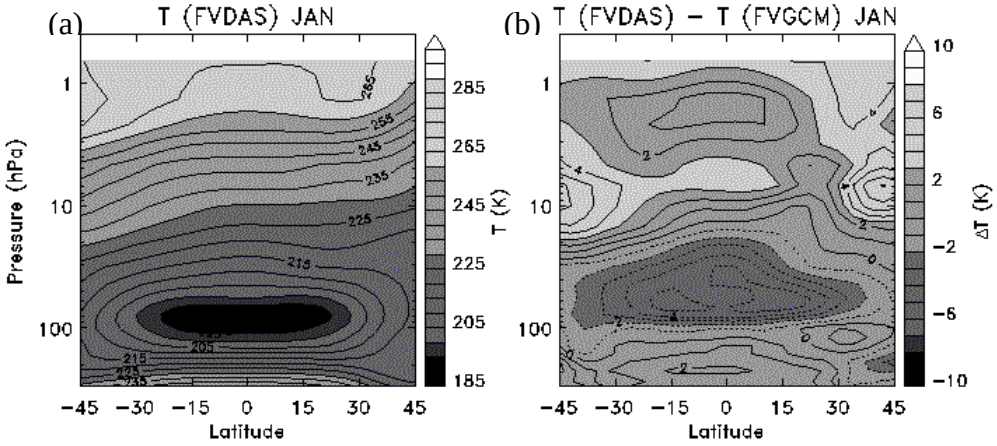

Figure 3 (a) The January zonal mean temperature for FVDAS and (b) the difference between the January zonal mean temperature from FVDAS and FVGCM.

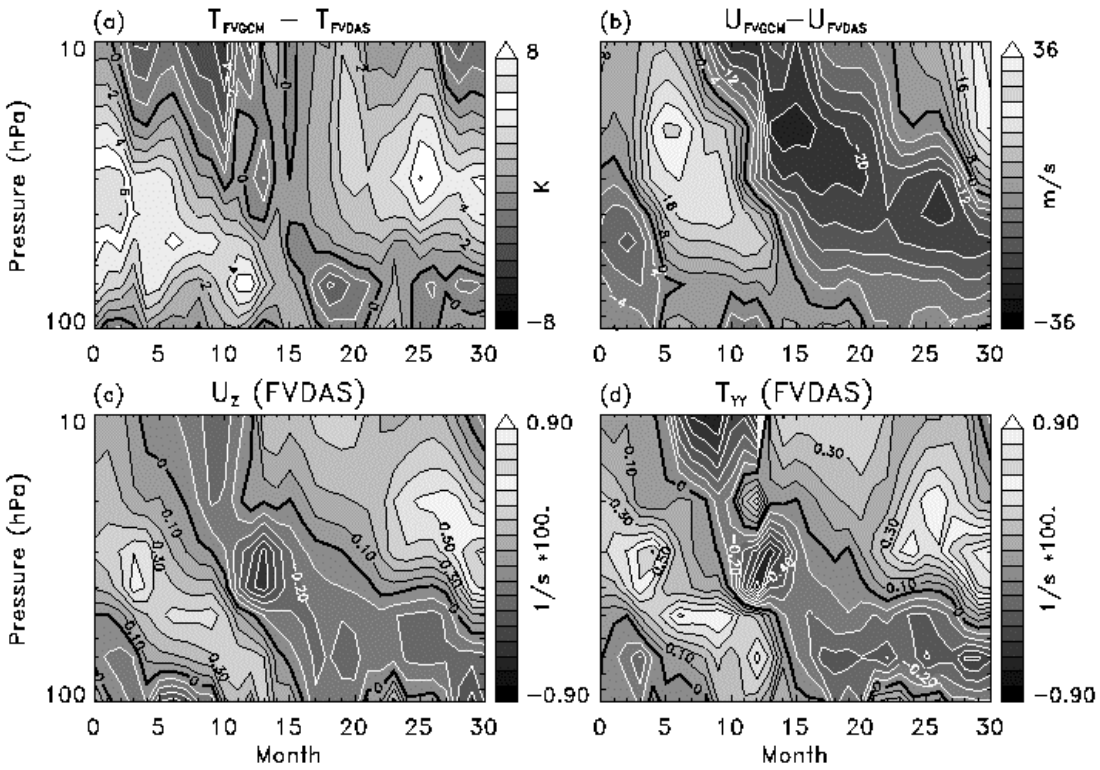

Figure 4 Time series at the equator show that winds and temperatures from FVGCM are rarely similar to those from FVDAS. (a) $\Delta T = T_{FVGCM} - T_{FVDAS}$; (b) $\Delta U = U_{FVGCM} - U_{FVDAS}$. The fields from FVDAS satisfy the equatorial thermal wind relationship (equation 1): (c) the vertical derivative of the zonal mean wind (left side of equation 1); (d) the right side of equation 1 calculated for zonal mean temperature. The implicit forcing derived from the observations through the assimilation system to produce the QBO signature in the temperature and wind fields from FVDAS represents physical processes that are absent from FVGCM.

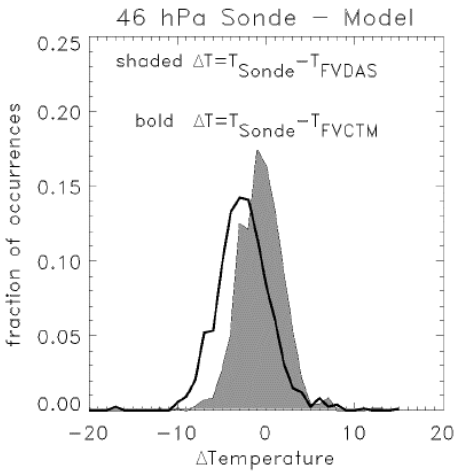

Figure 5 Temperatures at 46 hPa from the SHADOZ sondes are compared with those from FVDAS and from FVGCM. A histogram of ΔT = sonde temperatures - T_{FVGCM} (bold line) shows a negative bias; the mean difference is –2.13K The histogram ΔT = sonde temperatures – T_{FVDAS} (shaded) shows almost no bias; the mean difference is –0.11K. The standard deviation of the distribution sonde temperatures - T_{FVDAS} (3.03K) is smaller than sonde temperatures - T_{FVGCM} (3.52K).

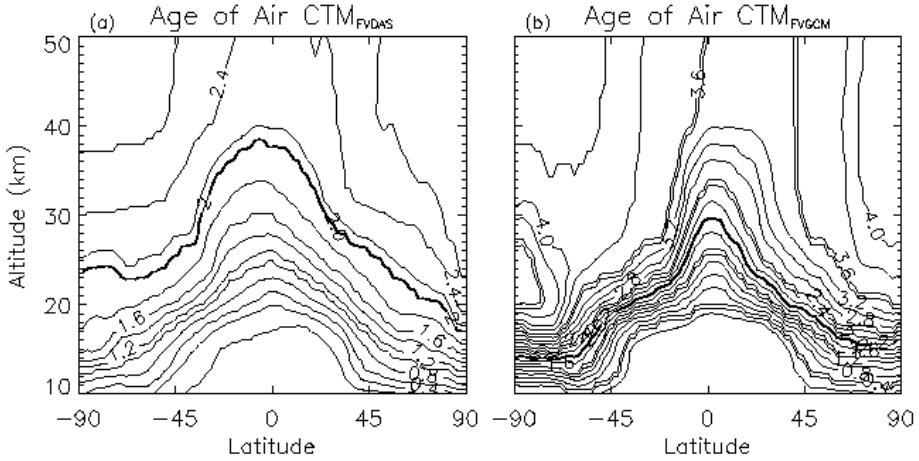

Figure 6 (a) Age of air calculated from an SF-6 simulation using CTM_{FVDAS}. The age calculation converges after 5 years integration. (b) Same as (a) but using CTM_{FVGCM}. The age calculation converges after 9 years integration. The contour interval is 0.2 years; the 2 year contour is bold for both panels.

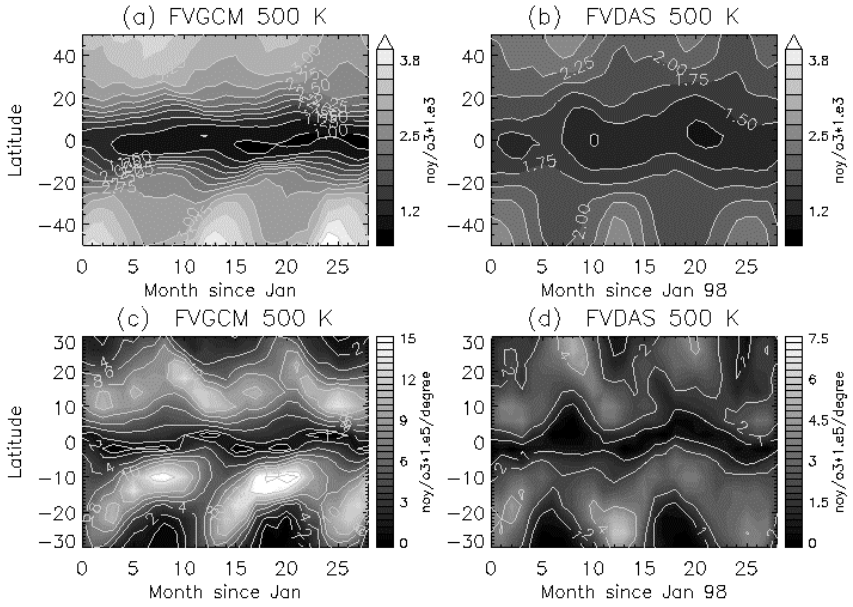

Figure 7 Time series at 500 K of the ratio NO_y/O_3 * 1.e3 (a) calculated using CTM_{FVGCM} winds; (b) calculated using CTM_{FVDAS} winds. Time series at 500K of the latitudinal derivative of NO_y/O_3*1.e3 (c) calculated using CTM_{FVGCM}; (d) calculated using CTM_{FVDAS}. Note that the range of values in (c) is twice the range of values in (d). In both (c) and (d), the latitude of the steepest gradient in the northern hemisphere during fall is poleward of its spring location.

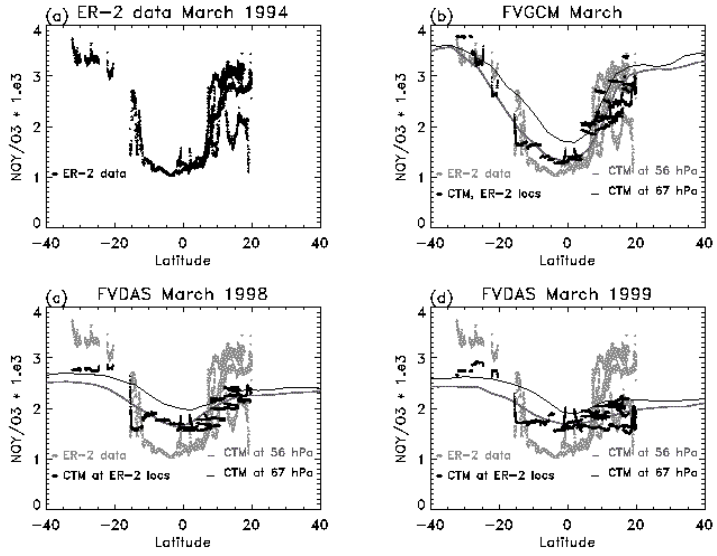

Figure 8 (a) ER-2 observations of NO_y/O_3 * 1.e3; (b) ER-2 observations (grey) and model values (black) of NO_y/O_3 * 1.e3 at locations of ER-2 observations. The solid lines are the model zonal average NO_y/O_3 *1.e3 at 67 hPa (thin) and 57 hPa (bold).

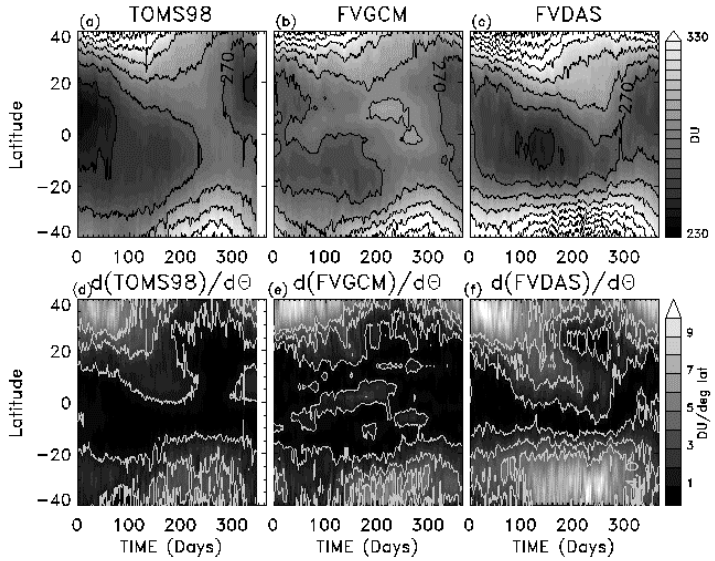

Figure 9 Time series of total zonal mean total ozone from (a) TOMS; (b) CTM_{FVGCM}; (c) CTM_{FVDAS}, and of the absolute value of the latitudinal derivative from (d) TOMS; (e) CTM_{FVGCM} (f) CTM_{FVDAS}. The bold line indicates 1DU/^{o}lat; the area enclosed by these contours exhibits weak gradients.

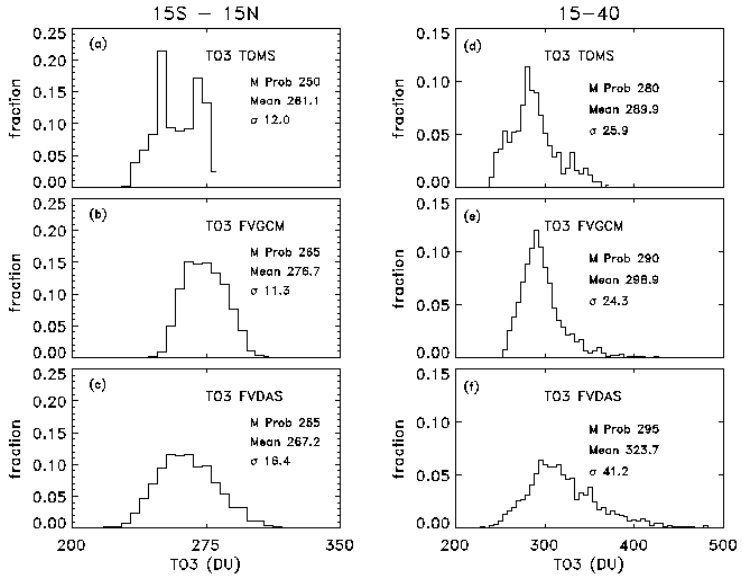

Figure 10 Distribution functions (a) 1998 TOMS observations between 15S and 15N; (b) same as (a) for model total ozone using FVDAS; (c) same as (a) for model total ozone using FVGCM; (d) same as (a) for 15-40N and 15-40S; (e) same as (d) for model total ozone using FVDAS; f) same as (d) for model total ozone using FVCTM.

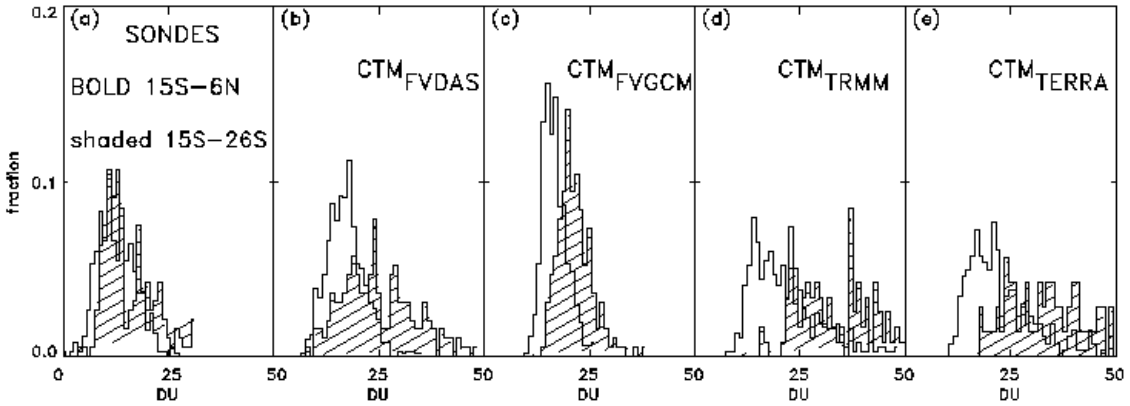

Figure 11 Distribution functions for the partial ozone column 140 hPa – 56 hPa (a) calculated from sondes; (b) model ozone using CTM_{FVDAS}; (c) model ozone using CTM_{FVGCM}; (d) model ozone using CTM_{TRMM}; (e) model ozone using CTM_{TERRA}. The bold line is the distribution for sonde locations between 14°S and 5.8°N; the shaded distribution is for sonde locations between 18°S and 26°S. Model values are at sonde locations.

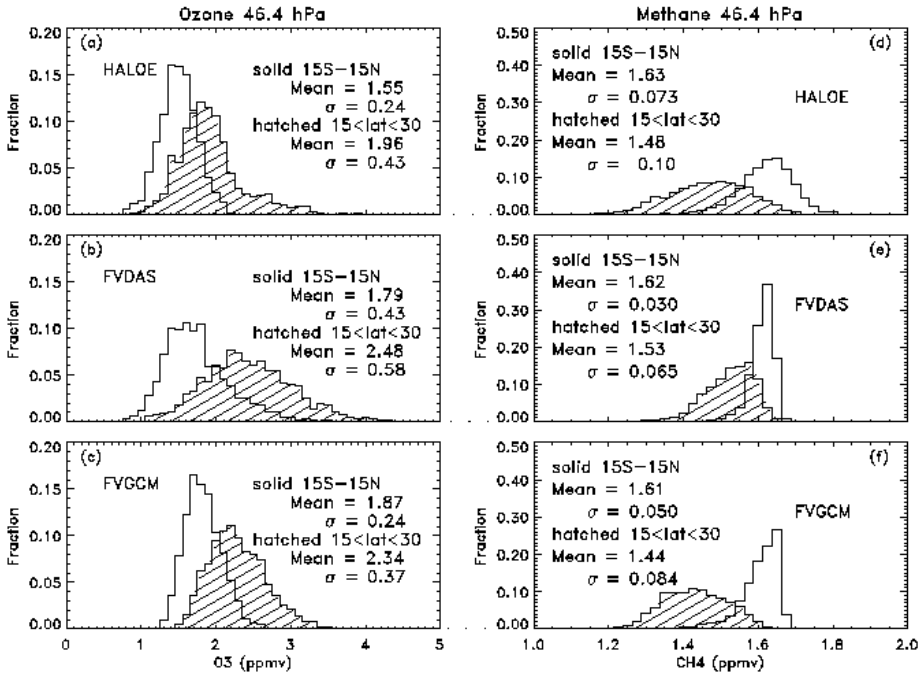

Figure 12 Probability distribution functions for (a) HALOE Ozone for observations between 15S and 15N (solid) and for latitudes between 15 and 30 (shaded); (b) same as (a) for ozone from CTM_{FVDAS} sampled as by HALOE; (c) same as (b) for ozone from CTM_{FVGCM}; (d) same as (a) for HALOE methane; (e) same as (b) for methane from CTM_{FVDAS} (f) same as (e) for methane from CTM_{FVGCM}.

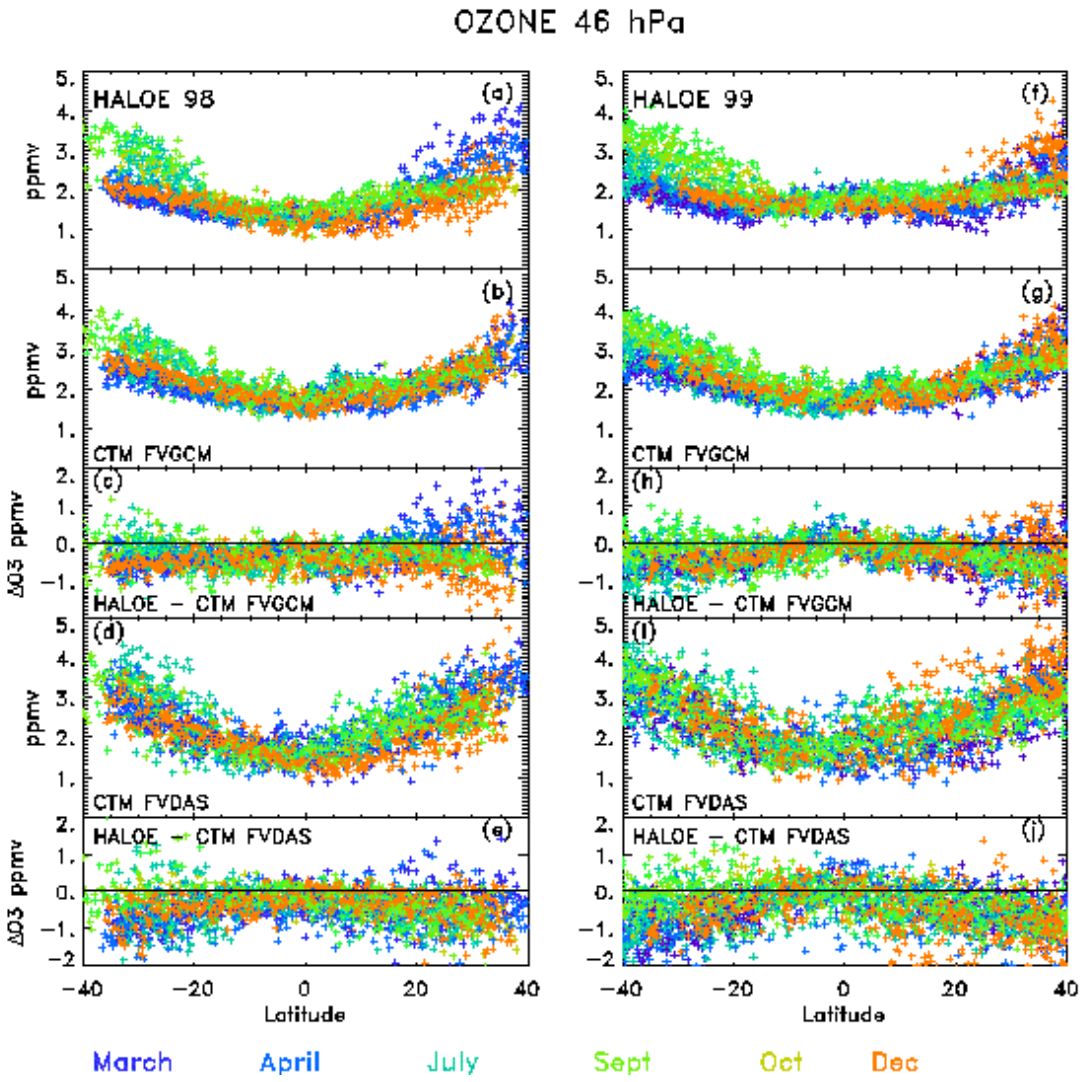

Plate 1 (a) HALOE O_3 for 1998 at 46 hPa organized by "sweeps"; each color refers to the month during which the HALOE observations were made as shown on the bottom of the figure; (b) CTM_{FVGCM} ozone for 1998 (c) $\Delta O_3 = O_{3(HALOE)} - O_{3(CTMFVGCM)}$ for 1998; (d) same as (b) for ozone from CTM_{FVDAS}; (e) $\Delta O_3 = O_{3(HALOE)} - O_{3(CTMFVDAS)}$ for 1998; (f) – (j) same as (a) – (e) for 1999.

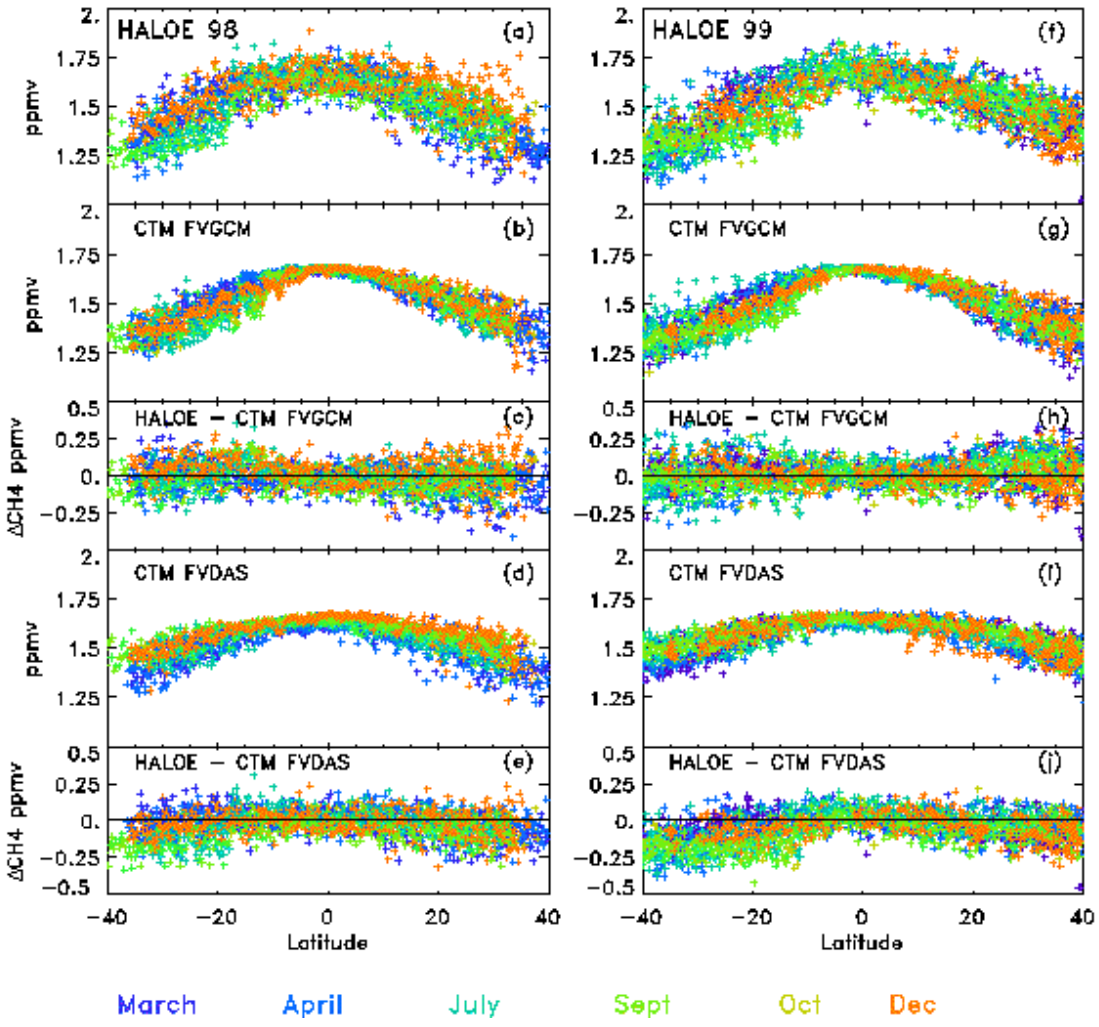

Plate 2 (a) HALOE CH_4 for 1998 at 46 hPa organized by "sweeps"; each color refers to the month during which the HALOE observations were made as shown on the bottom of the figure; (b) CTM_{FVGCM} methane for 1998; (c) $\Delta CH_4 = CH_{4(HALOE)} - CH_{4(CTMFVGCM)}$ for 1998; (d) same as (b) for methane from CTM_{FVDAS}; (e) $\Delta CH_4 = CH_{4(HALOE)} - CH_{4(CTMFVDAS)}$ for 1998; (f) – (j) same as (a) – (e) for 1999.

References

Anderson, D. E., Jr., and S. A. Lloyd, Polar twilight UV-visible radiation field: perturbations due to multiple scattering, ozone depletion, stratospheric clouds, and surface albedo, *J. Geophys. Res., 95,* 7429-7434, 1990.

Avallone L. M., and M. J. Prather, Photochemical evolution of ozone in the lower tropical stratosphere, *J. Geophys. Res., 101,* 1457-1461, 1996

Bey I., Jacob D. J., Yantosca R. M., Logan J. A., Field B. D., Fiore A. M., Li Q. B., Liu H. G. Y., Mickley L. J. , Schultz M. G., Global modeling of tropospheric chemistry with assimilated meteorology: Model description and evaluation, *J. Geophys. Res.,106,* 23,073-23,095, 2001.

Bloom, S. C., L. L. Takacs, A. M. DaSilva and D. Ledvina, Data assimilation using incremental analysis updates, *Mon. Wea. Rev., 124,* 1256-1271, 1996.

Brühl, C. et al., Halogen Occulation Experiment ozone channel validation, *J. Geophys. Res., 101,* 10,217-10,240, 1996.

Chin M., Rood R. B., Lin S. J., Muller J. F., Thompson A. M., Atmospheric sulfur cycle simulated in the global model GOCART: Model description and global properties, *J. Geophys. Res., 105,* 24,671-24,687, 2000

Chipperfield, M. P., D. Cariolle, P. Simon, A 3D chemical transport model study of chlorine activation during EASOE, *Geophys. Res. Lett. 21,* 1467-1470, 1994.

Chipperfield, M. P., M. L. Santee, L. Froidevaux, G. L. Manney, W. g. Read, J. W. Waters, A. E. Roche, and J. M. Russell, Analysis of UARS data in the southern polar vortex in September 1992 using a chemical transport model, *J. Geophys. Res., 101,* 18,861-18,881, 1996.

Chipperfield, M. P and J. A. Pyle, Model sensitivity studies of Arctic ozone depletion, *J. Geophys. Res., 103*, 28,389-28,403, 1998.

Chipperfield, M. P., and R. L. Jones, Relative influences of atmospheric chemistry and transport on Arctic ozone trends, *Nature, 400*, 551-554, 1999.

Chipperfield, M. P., Multiannual simulations with a three-dimensional chemical transport model, *J. Geophys. Res., 104*, 1781-1806, 1999.

Cohn, S.E., A. da Silva, J. Guo, M. Sienkiwiecz, and D. Lamich, Assessing the Effects of Data Selection with the DAO Physical-Space Statistical Analysis System. *Mon. Weath. Rev.*, **126**, 2913-2926, 1998.

Considine, D. B., S. R. Kawa, M. R. Schoeberl, and A. R. Douglass, N_2O and NO_y observations in the 1999/2000 Arctic polar vortex: Implications for transport processes in a CTM, *submitted to J. Geophys. Res.*, 2002.

Dee, D.P. and A. M. da Silva, Data assimilation in the presence of forecast bias, *Quart. J. Roy. Met. Soc., 124 Part A*, 269-295, 1998.

Dee, D. P., and R. Todling, Data assimilation in the presence of forecast bias: The GEOS moisture analysis, *Mon. Wea. Rev., 128*, 3268-3282, 2000.

Deniel, C., R. M. Bevilacqua, J. P. Pommereau, and F. Lefevre, Arctic chemical ozone depletion during the 1994-1995 winter deduced from POAM II satellite observations and the TRPROBUS three-dimensional model, *J. Geophys. Res., 103*, 19,231-19,244, 1998.

Douglass, A. R., R. Rood, J. Waters, L. Froidevaux, W. Read, L. Elson, M. Geller, Y. Chi, M. Cerniglia, S. Steenrod, A 3D simulation of the early winter distribution of reactive chlorine in the north polar vortex, Geophys. Res. Lett., 20, 1271-1274, 1993.

Douglass, A. R., R. B. Rood, S. R. Kawa and D. J. Allen, A three-dimensional simulation of the evolution of the middle latitude winter ozone in the middle stratosphere, J. Geophys. Res., 19,217-19,232, 1997.

Douglass, A. R., M. J. Prather, T. M. Hall, S. E. Strahan, P. J. Rasch, L. C. Sparling, L. Coy and J. M. Rodriguez, Choosing meteorological input for the global modeling initiative assessment of high-speed aircraft, *J. Geophys. Res.*, *104*, 27,545-27,564, 1999.

Eluszkiewicz, J., R. S. Hemler, J. D. Mahlman, L. Bruhwiler, and L. L. Takacs, Sensitivity of age-of-air calculations to choice of advection scheme, *J. Atmos. Sci., 57,* 3185-3201, 2000.

Fahey, D. W., K. K. Kelly, G. V. Ferry, L. R. Poole, J. C. Wilson, D. M. Murphy, M. Loewenstein and K. R. Chan, In-situ measurements of total reactive nitrogen, total water, and aerosol in polar stratospheric clouds in the Antarctic stratosphere, *J. Geophys. Res., 94*, 11299-11315, 1989.

Fahey, D. W., et al., *In situ* observations of NOy, O3, and the NOy/O3 ratio in the lower stratosphere, *Geophys. Res. Lett., 13,* 1653-1656, 1996.

Geller, M. A., V. Yudin, A. R. Douglass, J. W. Waters, L. S. Elson, A. E. Roche, and J. M. Russell III, UARS PSC, ClONO2, HCl and ClO measurements in early winter;

additional verification of the paradigm for chlorine activation, Geophys. Res. Lett., 22, 2937-2940, 1995.

Ginoux P., Chin M., Tegen I., Prospero J. M., Holben B., Dubovik O., Lin S. J., Sources and distributions of dust aerosols simulated with the GOCART model, *J. Geophys. Res.,106,* 20,255-20,273, 2001.

Goutail, R., et al., Depletion of column ozone in the Arctic during the winters 1993-94 and 1994-95, *J. Atmos. Chem., 32,* 1-34, 1999.

Griffith A. K. and N. K. Nichols, Adjoint methods in data assimilation for estimating model error, *Flow Turbulence and Combustion, 65,* 469-488, 2000.

Hall, T. M., and R. A. Plumb, Age as a diagnostic of stratospheric transport, *J. Geophys. Res., 99, 1059-1070,* 1994.

Hall T. M., D. W. Waugh, K. A. Boering, and R. A. Plumb, Evaluation of transport in stratospheric models, *J. Geophys. Res., 104,* 18,815-18,839, 1999.

Jackman, C. H., A. R. Douglass, K. F. Brueske, S. A. Klein, The Influence of dynamics on two-dimensional model reslts: simulations of ^{14}C and aircraft NO_x injections, *J. Geophys. Res., 96,* 22,559-22,572, 1991.

Joiner, J., and L. Rokke, Variational cloud-clearing with TOVS data, Q. J. Roy. Met. Soc., 196, 725-748 Part B 2000.

JPL, Chemical kinetics and photochemical data for use in stratospheric modeling, Evaluation Number 13, Sander, S. P., et al., eds., JPL Publication 00-3, 2000.

Kawa, S. R., R. Bevilacqua, J. J. Margitan, A. R. Douglass, M. R. Schoeberl, K. Hoppell, B. Sen, The interaction between dynamics and chemistry of ozone in the set-up phase of the northern hemisphere polar vortex, *J. Geophys. Res., in press,* 2002.

Kiehl, J.T., J.J. Hack, G.B. Bonan, B.A. Boville, D.L. Williamson, and P.J. Rasch, The National Center for Atmospheric Research Community Climate Model: CCM3. *J. Climate*, **11**, 1131-1149, 1998.

Ko, M. K. W., Nien-Dak Sze and D. K. Weisenstein, The roles of dynamical and chemical processes in determining the stratospheric concentration of ozone in one-dimensional and two-dimensional models, *J. Geophys. Res.*, *94*, 9889-9896, 1989.

Kondo, Y., S. R. Kawa, D. Lary, T. Sugita, A. R. Douglass, E. Lutman, M. Koike, and T. Deshler, Interpretation of nitric oxide profile observed in January 1992 over Kiruna, *J. Geophys. Res.*, *101*, 12,555-12,566, 1996.

Lefèvre, F., G. P. Brasseur, I. Folkins, A. K. Smith, and P. Simon, Chemistry of the 1991-1992 stratospheric winter: Three-dimensional model simulations, *J. Geophys. Res.*, *99*, 8183-8196, 1994.

Lin, S. J., and R. B. Rood, Multidimensional flux form semi-Lagrangian transport schemes, *Mon. Wea. Rev.*, *124*, 2046-2070, 1996.

Lin, S.-J., A Finite-Volume Integration Scheme for Computing Pressure-Gradient Forces in General Vertical Coordinates. *Q. J. R. Meteorol. Soc.*, **123**, 1749-1762, 1997.

Lin, S.-J., and R.B. Rood, An explicit flux-form semi-Lagrangian shallow-water model on the Sphere. *Q. J. R. Meteorol. Soc.*, **124**, 2477-2498, 1997.

McPeters, R. D., et al., Earth Probe Total Ozone Mapping Spectrometer (TOMS) Data Products User's Guide, NASA Reference Publication , Goddard Space Flight Center, Greenbelt MD 20771, 1998.

Park J. H., M. K. W. Ko, C. H. Jackman, R. A. Plumb, J. A. Kaye, K. H .Sage, Models and Measurements Intercomparison II, NASA/TM-1999-209554, 1999.

Park, J. H., et al., Validation of Halogen Occultation Experiment CH4 measurements from the UARS, *J. Geophys. Res., 101,* 10,183-10,205, 1996.

Plumb, R.A., A "tropical pipe" model of stratospheric transport, *J. Geophys. Res., 101, 3957-3972,* 1996.

Profitt, M. H., M. J. Steinkamp, J. A. Powell, R. J. McLaughlin, O. A. Mills, A. L Schmeltekopf, T. L. Thompson, A. F. Tuck, T. Tyler and R. H. Winkler, In situ ozone measurements within the 1987 Antarctic ozone hole from a high-altitude ER-2 aircraft, *J. Geophys. Res., 94,* 16547-16555, 1989.

Rood, R. B., D. J. Allen, W. E. Baker, D. J. Lamich and J. A. Kaye, The use of assimilated stratospheric data in constituent transport calculations, *J. Atmos. Sci., 46,* 687-701, 1989.

Rood, R. B., A. R. Douglass, J. A. Kaye, M. A. Geller, C. Yuechen, D. J. Allen, E. M. Larson, E. R. Nash, and J. E. Nielsen, Three-Dimensional simulations of wintertime ozone variability in the lower stratosphere, *J. Geophys. Res.,* 96, 5055-5071, 1991.

Russell J. M., L L. Gordley, J. H. Park, S. R. Drayson, W. D. Hseketh, R. J. Cicerone, A. F. Tuck, J. E. Frederick, J. E. Harries, and P. J. Crutzen, The Halogen Occultation Experiment, *J. Geophys. Res., 98,* 10,777-10,798, 1993.

Schoeberl, M. R., A. R. Douglass, Z. Zhu, and S. Pawson, A Comparison of the lower stratospheric age-spectra derived from a general circulation model and two data assimilation systems, submitted to *J. Geophys. Res.,* 2002.

Sinnhuber, B.-M., M. P. Chipperfield, S. Davies, J. P. Burrows, K.-U. Eichmann, M. Weber, P. von der Gathen, G. A. Cahill, A. M. Lee, J. A. Pyle, Large loss of total ozone during the Arctic winter of 1999/2000, *Geophys. Res. Lett., 27,* 3473-3476, 2000.

Stolarski, R. S., et al. 1995 scientific assessment of the atmospheric effects of stratospheric aircraft, *NASA Ref. Publ. 1381,* 1995.

Trepte, C. R., and M. H. Hitchman, Tropical stratospheric circulation deduced from satellite aerosol data, *Nature , 355,* 626-628, 1992.

Thompson, A.M., et al., The 1998-2000 SHADOZ (Southern Hemisphere Additional Ozonesondes) Tropical Ozone Climatology. 1. Comparisons with TOMS and Ground-based Measurements, J. *Geophys. Res., in press,* 2002.

Waugh, D. W., Seasonal variation of isentropic transport out of the tropical stratosphere, *J. Geophys. Res., 101,* 4007-4023, 1996.

Weaver, C. J., A. R. Douglass, D. b. Considine, A 5-year simulation of supersonic aircraft emission transport using a three-dimensional model, *J. Geophys. Res., 101,* 20,975-20,984, 1996.

Weaver, C. J., A. R. Douglass and R. B. Rood, Lamination frequencies as a diagnostic for horizontal mixing in a 3D transport model, *J. Atmos. Sci., 57,* 247-261, 2000.

Wennburg, P. O., et al., The removal of lower stratospheric O_3 by free radical catalysis: *in situ* measurements of OH, HO_2, NO, NO_2, ClO and BrO, *Science, 266,* 398-404, 1994.